1-1-1996

Modeling The Post-Burn-In Abnormal Base Current In Algaas/Gaas Heterojunction Bipolar Transistors

S. Sheu
University of Central Florida

J. J. Liou
University of Central Florida

C. I. Huang

D. C. Williamson

Journal of
Applied Physics

Modeling the post-burn-in abnormal base current in AlGaAs/GaAs heterojunction bipolar transistors

Cite as: Journal of Applied Physics **79**, 7348 (1996); https://doi.org/10.1063/1.361451
Submitted: 24 July 1995 . Accepted: 24 January 1996 . Published Online: 04 June 1998

S. Sheu, J. J. Liou, C. I. Huang, and D. C. Williamson

Modeling the post-burn-in abnormal base current in AlGaAs/GaAs heterojunction bipolar transistors

S. Sheu and J. J. Liou
Electrical and Computer Engineering Department, University of Central Florida, Orlando, Florida 32816

C. I. Huang
Device Technology Division, Wright Laboratory, Wright-Patterson AFB, Ohio 45433

D. C. Williamson
Electromagnetic and Reliability Directorate, Rome Laboratory, Griffiss AFB, New York 13422

(Received 24 July 1995; accepted for publication 24 January 1996)

The base current of AlGaAs/GaAs heterojunction bipolar transistor subjected to a long burn-in test often exhibits an abnormal characteristic with an ideality factor of about 3, rather than a normal ideality factor between 1 and 2, in the midvoltage range. We develope an analytical model to investigate the physical mechanisms underlying such a characteristic. Consistent with the finding of an experimental work reported recently, our model calculations show that the recombination current in the base has an ideality factor of about 3 in the midvoltage range and that such a current is responsible for the observed abnormal base current in heterojunction bipolar transistor after a long burn-in test. Post-burn-in data measured from two different heterojunction bipolar transistors are also included in support of the model. © *1996 American Institute of Physics.*
[S0021-8979(96)07609-7]

I. INTRODUCTION

Burn-in tests carried out in a thermal and/or electrical stress condition are useful in determining the long-term performance of AlGaAs/GaAs heterojunction bipolar transistors (HBTs).[1–3] Experimental results often show that the burn-in test increases considerably the base current I_B but does not alter notably the collector current I_C. Furthermore, an abnormal base current with an ideality factor $n \approx 3$ in the midvoltage range is often observed in the Gummel plot of a HBT subjected to a relatively long-hour burn-in test.[1–3] An attempt has been made earlier to model the HBT post-burn-in behavior.[4] The analysis was based on the theory that the defects at the base surface may migrate to the heterointerface during the high thermal/electrical stress condition (i.e., recombination/thermal enhanced defect diffusion[5]). While such a model can successfully describe I_B and I_C in HBTs subjected to a relative short burn-in test (I_B and I_C after 144 h stress shown in Fig. 1), it fails to predict I_B with $n \approx 3$ characteristics observed in the HBT after a long-hour stress test, as evidenced by the results of I_B measured after 300 h stress given in Fig. 1. Sugahara *et al.*[3] have suggested that such an abnormal current can be attributed to a significant increase in the number of defects in the strained base (i.e., stress-induced defects) during the long stress hours. Also, they have demonstrated that the post-burn-in I_B can be greatly reduced if the base lattice strain is relaxed.

This article presents a comprehensive theoretical study on the abnormal base current in the post-burn-in HBT. Based on the Shockley–Read–Hall (SRH) recombination statistics, a model for the recombination current in the base region is developed. Our model calculations show that such a current has an ideality factor of about 3 in the midvoltage range and thus is responsible for the observed abnormal base current in HBT after a long burn-in test. With the aid of the model and measurement data, physical mechanisms underlying the observed abnormal base current in the post-burn-in HBT are also discussed.

II. MODEL DEVELOPMENT

A. Pre-burn-in HBT

We focus on the base current of a mesa-etched $N/p^+/n$ HBT. There are two major components for the base current of pre-burn-in HBT,

$$I_B = I_{\mathrm{BL}} + I_{\mathrm{BN}}, \tag{1}$$

where I_{BL} is the base leakage current and I_{BN} is the normal base current. For the bias condition of applied base-collector voltage $V_{\mathrm{CB}}=0$ and base-emitter voltage $V_{\mathrm{BE}}>0$ (i.e., forward-active mode), the base leakage current is originated from the leakage of electron from the base to emitter through the emitter-base periphery and is the dominate current component for I_B at relatively small V_{BE}.[6] This current is given by[6]

$$I_{\mathrm{BL}} = P_E J'_{\mathrm{BL}}[1 - \exp(-V_{\mathrm{BE}} F_L / V_T)], \tag{2}$$

where P_E is the emitter perimeter length, J'_{BL} is the fully activated (i.e., $V_{\mathrm{BE}} \gg V_T$) base leakage current density, and F_L is an empirical parameter determining the shape of the base leakage current.

The normal base current in general consists of:

(1) the recombination current I_{SCRE} in the emitter side of the heterojunction space-charge region;
(2) the recombination current I_{SCRB} in the base side of the heterojunction space-charge region;
(3) the surface recombination current I_{RS} at the emitter side walls and extrinsic base surface;
(4) the recombination current I_{QNB} in the QNB; and
(5) the injection current I_{RE} from the base into emitter.

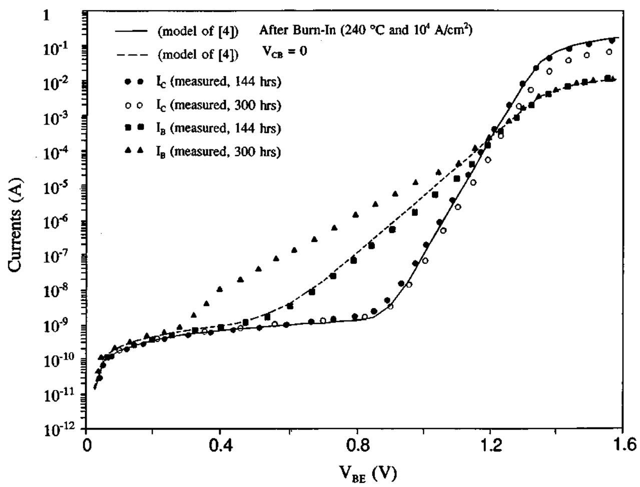

FIG. 1. Base and collector current characteristics of a post-burn-in (subjected to 240 °C temperature and 10^4 A/cm^2 current density stress) AlGaAs/GaAs HBT calculated from a previously developed model Ref. 4 and obtained from measurements. The model of Ref. 4 gives an accurate prediction for the HBT behavior after a relatively short stress test (i.e., 144 h), but fails to describe the base current (i.e., with an ideality factor of about 3 between V_{BE}=0.3 and 1.2 V) of the HBT subjected to a long stress test (i.e., 300 h).

The details of these current components can be been found in the literature.[7] For pre-burn-in HBTs, I_{QNB} is negligible because the number of defects in the QNB is small and the base is very thin. In addition, I_{SCRB} is neglected due to the fact that the majority of the space-charge region (SCR) resides in the emitter because of the very high base doping density. Thus,

$$I_{BN}=I_{SCRE}+I_{RS}+I_{RE}. \tag{3}$$

The ideality factor of this current ranging from 1 to 2.

B. Post-burn-in HBT

After a long burn-in test, the number of defects in the base will be increased significantly due to the strained lattice during the stress test.[3] As a result, substantial electron–hole recombination occurs in both the base side of the SCR and the QNB, and the conventional thin QNB and thin SCR approximations are no longer valid. Thus, for a HBT after a long burn-in test,

$$I_{BN}=I_{BASE}+I_{SCRE}+I_{RS}+I_{RE}, \tag{4}$$

where $I_{BASE}=I_{SCRB}+I_{QNB}$, and

$$I_{BASE}=Aq\int_0^{X_2}U^{SRH}(x)dx+Aq\int_{X_2}^{X_B}U^{SRH}(x)dx. \tag{5}$$

Here A is the emitter area, $x=0$ and X_2 are the boundaries of base-side SCR, $x=X_2$ and X_B are the boundaries of the QNB, and U^{SRH} is the total SRH recombination rate summing the recombination rates at each trapping state E_{Ti} ($i=1,2,\ldots,N$, N is the total number of trapping states),

$$U^{SRH}=\sum_{i=1}^{N} U_i^{SRH}, \tag{6}$$

and[7]

$$U_i^{SRH}=(pn-n_i^2)(1+\Gamma)(N_{Ti}\sigma_i v_{th})\{p+n+2n_i \times\cosh[(E_{Ti}-E_i)/kT]\}^{-1}. \tag{7}$$

p and n are hole and electron concentrations in the QNB, n_i is the intrinsic free-carrier concentration, Γ is the trap-assisted tunneling factor, N_{Ti} is the trapping density at E_{Ti}, σ_i ($\approx 10^{-14}$ cm^{-2}) is the capture cross section at N_{Ti}, v_{th} ($\approx 10^7$ cm/s) is the electron thermal velocity, and E_i is the intrinsic Fermi energy. The trap-assisted tunneling is important for the high-field region, such as the emitter-base SCR, where electrons can tunnel through the energy band via traps and subsequently recombine with holes.[8] In a low-field region, such as the QNB, Γ approaches zero. This factor is given by[8]

$$\Gamma=\left(\frac{\Delta E}{kT}\right)\int_0^1 \exp\left(\frac{u\Delta E}{kT}-K'u^{1.5}\right)du. \tag{8}$$

Here ΔE is the energy between the conduction-band edge and the trapping state energy since electrons in these energies are tunneling possible, and K' is a parameter inversely proportional to the local electric field ξ,

$$K'=(4/3)(2m^*\Delta E^3)^{0.5}/(q\hbar\xi). \tag{9}$$

m^* is the effective electron mass and $\hbar$ is the reduced Planck constant. When ξ is large, K' is small, and Γ becomes large.

For the QNB, the minority-carrier lifetime τ_B is related to the electron concentration as[9]

$$\tau_B=(n-n_0)/U^{SRH}=\Delta n/U^{SRH}, \tag{10}$$

where n_0 is the equilibrium electron concentration and Δn is the excess electron concentration. For a base with an arbitrary length,[7]

$$\Delta n=\Delta n(X_2)\sinh[(X_B-x)/L_n]/\sinh[(X_B-X_2)/L_n]. \tag{11}$$

Here $L_n=(D_n\tau_B)^{0.5}$ is the electron diffusion length in the QNB and, using the thermionic and tunneling mechanisms at heterointerface and Boltzmann statistics in the QNB,[10]

$$\Delta n(X_2)=qv_n\gamma_n N_E\exp(-V_{B1}/V_T)/\zeta, \tag{12}$$

$$\zeta=qD_n/(X_B-X_2+D_n/v_s)+qv_n\gamma_n \times\exp[(V_{B2}-\Delta E_C/q)/V_T], \tag{13}$$

where v_n is the electron thermal velocity, γ_n is the electron tunneling coefficient, N_E is the emitter doping concentration, and V_{B1} and V_{B2} are the barrier potentials on the emitter and base sides of the junction, respectively. Since τ_B and Δn are related to each other, a numerical procedure is needed to calculate U_{SRH}, and thus I_{QNB}, iteratively, provided the parameters associated with the SRH process (i.e., E_{Ti}, N_{Ti}, and N) are specified.

For the SCR, n, p, and ξ distributions in the base side of SCR needed in Eqs. (7) and (8) are given by

$$n(x)=n(X_2)\exp[-V_i(x)/V_T], \tag{14}$$

$$p(x)=p(X_2)\exp[V_i(x)/V_T], \tag{15}$$

$$\xi(x)=-(qN_B/\epsilon_B)(X_2-x) \tag{16}$$

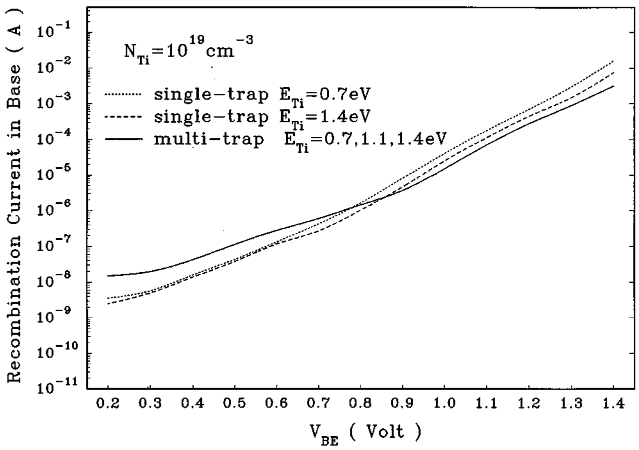

FIG. 2. Recombination current in the base vs V_{BE} calculated from the model for three different cases of N_{Ti} and N.

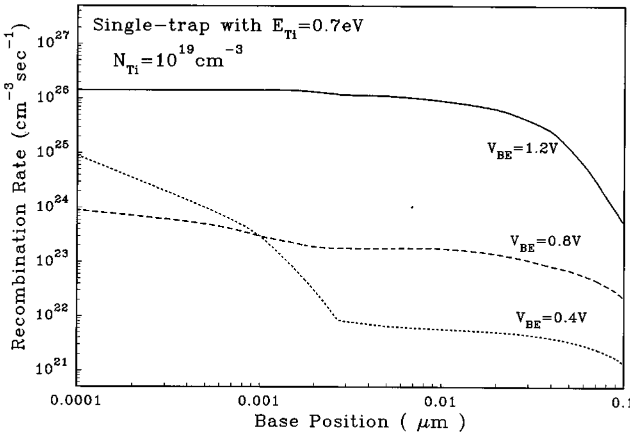

FIG. 4. SRH recombination rates vs base position calculated for three different V_{BE}.

where V_i is the electrostatic potential [i.e., $V_i(X_2)=0$ is chosen as the reference potential], N_B is the base doping concentration, and ϵ_B is the dielectric permittivity in base. The position-dependent V_i in the base side of SCR can be expressed as[7]

$$V_i(x)=-0.5(qN_B/\epsilon_B)(X_2-x)^2. \tag{17}$$

As is shown later, I_{BASE} has an ideality factor of about 3 in the midvoltage range and thus is the current component contributing to the abnormal base current observed in the post-burn-in HBT.

III. RESULTS AND DISCUSSIONS

We first investigate the effects of E_{Ti} and N on the recombination current in the base. The device considered has a typical makeup of 5×10^{17} cm^{-3} emitter doping concentration, 0.15 μm emitter layer thickness, 10^{19} cm^{-3} base doping concentration, and 0.1 μm base layer thickness. Also, the conduction-band edge E_C has been chosen as the reference for E_{Ti} (i.e., $E_{Ti}=0$ if located at E_C). Three different E_{Ti} of 0.7, 1.1, and 1.4 eV will be considered to represent various trapping state locations in the band gap (i.e., deep-, intermediate-, and shallow-level trapping states). Furthermore, only E_{Ti} below E_i are considered because only these types of E_{Ti} are important to trap-assisted tunneling in the base side of the SCR.[8] As is shown later, this is a major mechanism contributing to the abnormal base current.

Figure 2 shows I_{BASE} calculated from the model using fixed $N_{Ti}=10^{19}$ cm^{-3} and a single trap with $E_{Ti}=0.7$ eV, a single trap with $E_{Ti}=1.4$ eV, and multiple traps with $E_{Ti}=0.7$, 1.1, and 1.4 eV (i.e., $N=3$). The results suggest that I_{BASE} is relatively insensitive to E_{Ti}, but depends more on the number of trapping state N, particularly at small V_{BE}. Furthermore, all three currents exhibit an $n\approx3$ characteristic.

Intuitively, one expects I_{BASE} increases with increasing E_{Ti} and increasing N because U^{SRH} is inversely and directly proportional $\cosh(E_{Ti}/kT)$ and N [see Eqs. (6) and (7)], respectively. This is true for small V_{BE} (i.e., $V_{BE}<0.8$ V), where the electric field in the SCR is high, and recombination via trap-assisted tunneling in the SCR is the dominant process. For high V_{BE}, however, the electric field in the SCR is small, and the SRH recombination in the QNB is more

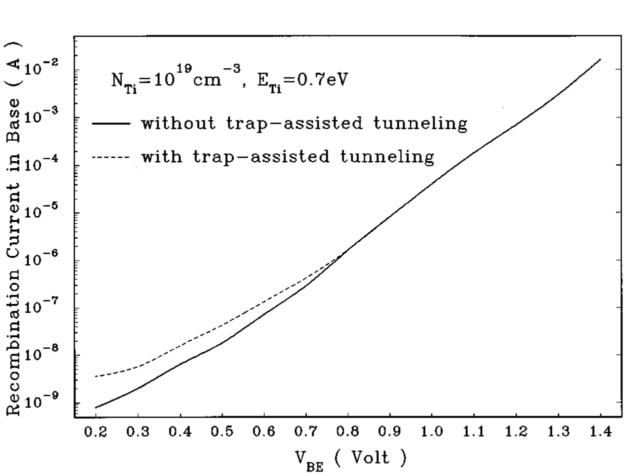

FIG. 3. Recombination current in the base calculated with and without the trap-assisted tunneling mechanism.

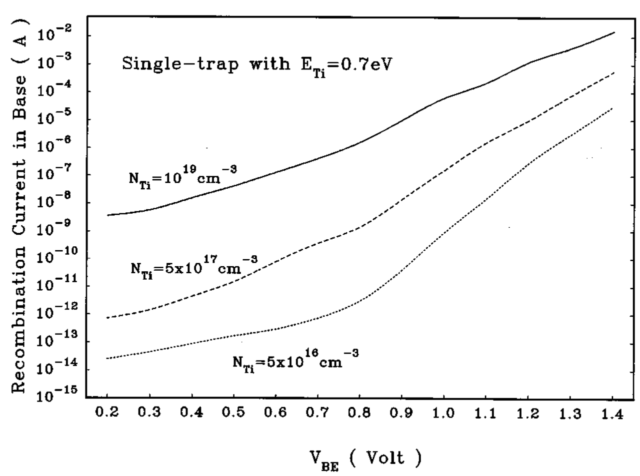

FIG. 5. Recombination current in the base vs V_{BE} calculated from the model for three different N_{Ti}.

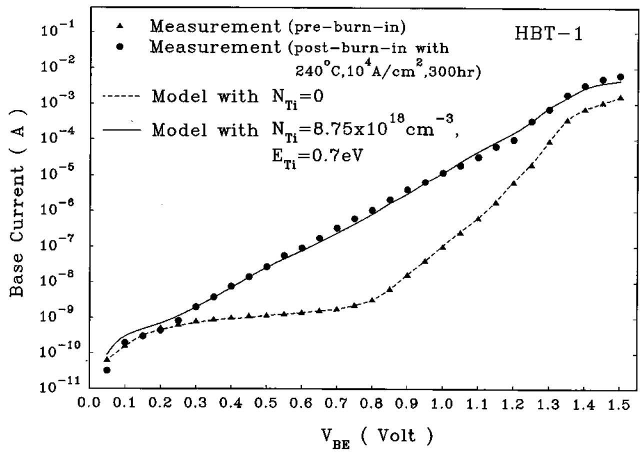

FIG. 6. Pre- and post-burn-in base currents of HBT-1 calculated from the model and obtained from measurements.

significant. Since U^{SRH} in the QNB is a function of the electron concentration, an increase in E_{Ti} and increase in N will tend to increase U^{SRH}, but such a change will also tend to decrease τ_B and therefore decrease the electron concentration and U^{SRH} in the QNB. This compensating mechanism leads to a less significant effect of E_{Ti} and N on I_{BASE}, as observed in the region of $V_{BE}>0.8$ V in Fig. 2. To further demonstrate this, we show in Fig. 3 I_{BASE} vs V_{BE} calculated with and without trap-assisted tunneling. It can be seen that the current component resulted from trap-assisted tunneling is negligible if V_{BE} is greater than 0.8 V. For this bias region, recombination current in the QNB is the dominant current, and I_{BASE} is less insensitive to N_{Ti} and N, as observed in Fig. 2. Also note that the abnormality of $n\approx 3$ is more evident in I_{BASE} with trap-assisted tunneling.

The dependence of $U^{SRH}(x)$ on V_{BE} is illustrated in Fig. 4. A logarithmic scale has been used for the x axis to illustrate the details of $U^{SRH}(x)$ in the base side of SCR (far left-hand side of the figure) due to trap-assisted tunneling. For relatively small V_{BE} (i.e., $V_{BE}=0.4$ and 0.8 V), the recombination rate in the SCR decreases with increasing V_{BE}

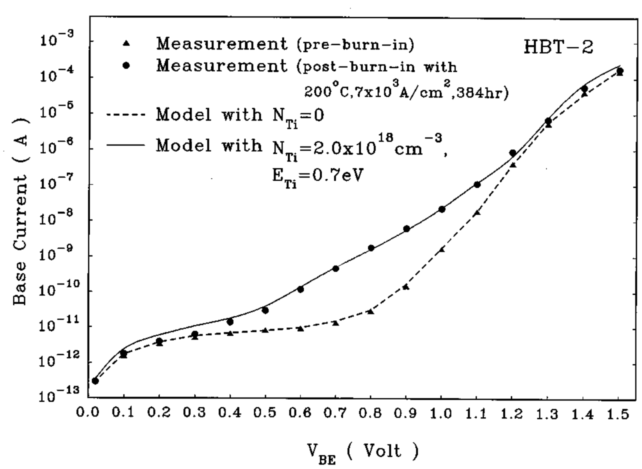

FIG. 7. Pre- and post-burn-in base currents of HBT-2 calculated from the model and obtained from measurements (Ref. 3).

TABLE I. HBT structures and leakage current parameters.

Parameters	HBT-1	HBT-2
Emitter doping (cm^{-3})	5×10^{17}	5×10^{17}
Emitter thickness (μm)	0.17	0.18
Emitter area (μm^2)	100	30
Base doping (cm^{-3})	1×10^{19}	1×10^{19}
Base thickness (μm)	0.1	0.14
J'_{BL} (A/cm)	1×10^{-5}	1.33×10^{-6}
F_L	0.005	0.005

because of a smaller electric field and thus a smaller trap-assisted tunneling factor in the region. The trend is reversed if V_{BE} is further increased (i.e., $V_{BE}=1.2$ V), however, due to the fact that the SCR is vanishing, and U^{SRH} becomes the QNB recombination rate.

Figure 5 shows the effect of N_{Ti} on the recombination current in the base. Here, we have arbitrarily chosen a single trap with $E_{Ti}=0.7$ eV in calculations. Clearly, the value of N_{Ti} affects I_{BASE} significantly, and N_{Ti} will be the main parameter in fitting the model calculations with experimental data.

Figure 6 shows the total base currents of pre- and post-burn-in HBT-1 (device makeup and its leakage current parameters are given in Table I) calculated from the model and obtained from measurements. The plateaulike current for $V_{BE}<0.8$ V in the pre-burn-in HBT is the base leakage current. For the post-stress HBT the current behavior for $V_{BE}>0.2$ V is changed to that of $n\approx 3$. This is due to the fact that, in addition to the base leakage current, there is a large I_{BASE} in the post-burn-in HBT. $N_{Ti}=8.75\times10^{18}$ cm^{-3} has been used to fit the model to measured data, suggesting the stress-induced defect density in such a HBT is 8.75×10^{18} cm^{-3}. A single trap with $E_{Ti}=0.7$ eV has also been used.

Figure 7 shows the total base currents of pre- and post-burn-in HBT-2 (see Table I) calculated from the model and obtained from measurements.[3] For this device, we found that the burn-in test resulted in $N_{Ti}=2\times10^{18}$ cm^{-3} in the base. This is smaller than N_{Ti} in HBT-1, due perhaps to the fact that HBT-2 is subjected to a less severe burn-in test (200 °C and 7×10^3 A/cm^2) than HBT-1 (240 °C and 10^4 A/cm^2).

IV. CONCLUSIONS

A model has been developed to investigate the physical mechanisms underlying the abnormal base current (i.e., with an ideality factor of about 3) observed in the post-burn-in AlGaAs/GaAs heterojunction bipolar transistor (HBT). Our study confirms the finding of recent experimental work that such a current resulted from the significant electron–hole recombination via stress-induced defect centers in the base of the HBT. Furthermore, it has been shown that the trap-assisted tunneling is an important mechanism for recombination in the space-charge region when the bias voltage is relatively low. The model calculations compare favorably with data measured from two different HBTs.

ACKNOWLEDGMENT

This work was supported in part by a research grant funded by the Air Force Office of Scientific Research.

[1] M. E. Hafizi, L. M. Pawlowicz, L. T. Tran, D. K. Umemoto, D. C. Streit, A. K. Oki, M. E. Kim, and K. H. Yen, in Digest of the IEEE GaAs IC Symposium, 1990, p. 329.
[2] T. Henderson, D. Hill, W. Liu, D. Costa, H. F. Chau, T. S. Kim, and A. Khatibzadeh, in Digest IEEE IEDM, 1994.
[3] H. Sugahara, J. Nagano, T. Nittono, and K. Ogawa, in Digest IEEE GaAs IC Symposium 1993, p. 115.
[4] J. J. Liou and C. I. Huang, Solid-State Electron. **37**, 1349 (1994).
[5] J. L. Benton, M. Levinson, A. T. Macrander, H. Temkin, and L. C. Kimerling, Appl. Phys. Lett. **45**, 566 (1984).
[6] J. J. Liou, C. I. Huang, B. Bayraktaroglu, D. C. Willamson, and K. B. Parab, J. Appl. Phys. **76**, 1349 (1994).
[7] For example, see J. J. Liou, *Advanced Semiconductor Device Physics and Modeling* (Artech, Boston, 1994).
[8] G. A. M. Hurkx, D. B. M. Klaassen, and M. P. G., IEEE Trans. Electron Devices **ED-39**, 331 (1992).
[9] C.-T. Sah, *Fundamentals of Solid-State Electronics* (World Scientific, Singapore, 1991), Chap. 3.
[10] M. S. Shur, *GaAs Devices and Circuits* (Plenum, New York, 1987).